

Hexakis(adamantyltrimethylammonium) cyclooctasilicate tetratetracontahydrate

Pieter L. H. Verlooy,^a Koen Robeyns,^{b,‡} Luc Van Meervelt,^b Christine E. A. Kirschhock^a and Johan A. Martens^{a*}

^aCentre for Surface Chemistry and Catalysis, Katholieke Universiteit Leuven, Kasteelpark Arenberg 23, B-3001 Leuven, Belgium, and ^bDepartment of Chemistry, Katholieke Universiteit Leuven, Biomolecular Architecture, Celestijnenlaan 200F, B-3001 Leuven, Belgium

Correspondence e-mail: johan.martens@biw.kuleuven.be

Received 27 June 2010

Accepted 31 October 2010

Online 19 November 2010

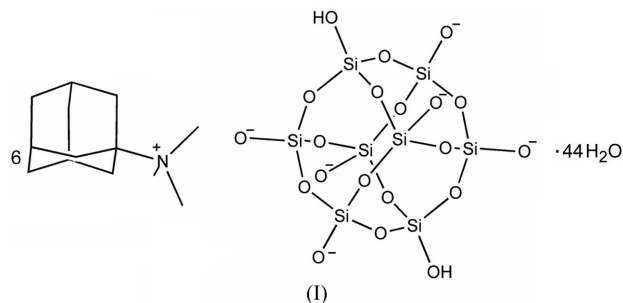
The title compound, $6C_{13}H_{24}N^+ \cdot H_2Si_8O_{20}^{6-} \cdot 44H_2O$, belongs to the class of cyclosilicate hydrates, which structurally can be positioned between the zeosils and the clathrate hydrates. $[Si_8O_{18}(OH)_2]$ cubes carrying six negative charges are located on crystallographic inversion centres and are surrounded by six adamantyltrimethylammonium cations.

Comment

In structural terms, silicate hydrates can be positioned between silicon dioxide-based zeolites, called zeosils, and silicate clathrate hydrates. In zeolites, (organic) template molecules are embedded in the pores of a four-connected silicon dioxide network. The template molecules reside in zero-, one-, two- or three-dimensional pores. In the crystal structures of clathrate hydrates, the template molecules are partially or entirely surrounded by water molecules. Silicate hydrates are crystalline materials consisting of water, individual silicate units and organic cations. The organic cations are embedded in cages or pores formed by a network of hydrogen-bonded water molecules and oligomeric silicate clusters (Wiebcke, 1991; Grube *et al.*, 1993).

The templates used to synthesize silicate hydrate materials can be subdivided into different groups (Verlooy *et al.*, 2010). The first group of organic templates consists of *N*-methyl quaternary amines [references 2–20 in Verlooy *et al.* (2010)], the second consists of the other quaternary amines [references 18 and 21–25 in Verlooy *et al.* (2010)] and the third comprises the metal–ethylenediamine complexes [references 26–30 in Verlooy *et al.* (2010)]. α -Cyclodextrine (Benner *et al.*, 1997)

and hexamethyleneimine (Verlooy *et al.*, 2010) are the only reported templates that do not fit this classification.



In the group of silicate hydrate materials synthesized with *N*-methyl quaternary amines, which form the majority of reported silicate hydrate materials, silicate cubes are surrounded by a shell of 24 water molecules. This observation is generally referred to as the ‘24-water rule’ (Wiebcke *et al.*, 1994). Another generally observed property of silicate hydrate structures is the relationship between the environment and the C/N ratio of the organic template molecules. Among all silicate hydrates reported to date, organic template molecules with a low C/N ratio were found to reside in one-dimensional pores. Organic template molecules with a high C/N ratio are generally found in two- or three-dimensional pore architectures (Smolin, 1970; Bissert & Liebau, 1987; Emmer & Wiebcke, 1994; Wiebcke *et al.*, 1995; Shantz & Lobo, 2001; Wiebcke & Felsche, 2001). So far no silicate hydrates with a C/N ratio higher than 10 have been synthesized (Wiebcke *et al.*, 1995; Shantz & Lobo, 2001).

We report here the title compound, (I), a silicate hydrate structure synthesized using an organic template with a C/N

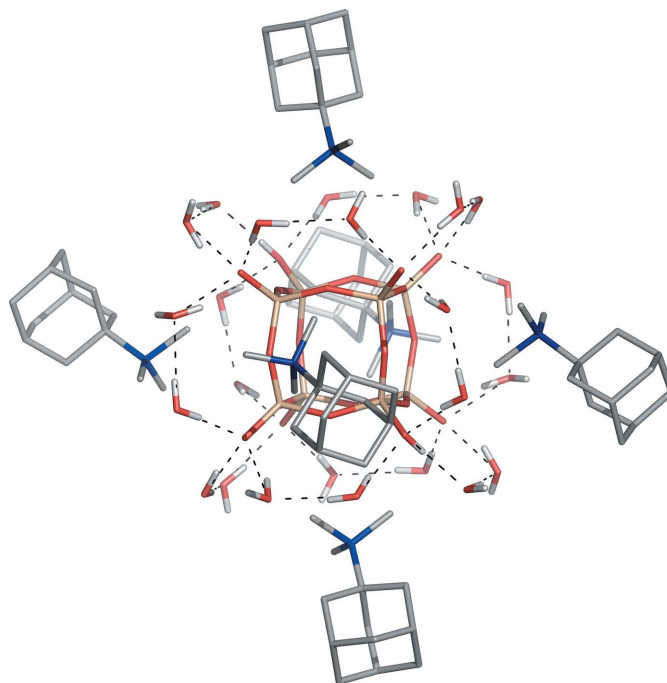


Figure 1
Stick representation of (I). Six TMA⁺ cations surround the silicate cage. For clarity, only water molecules in the first hydration shell are shown.

[‡] Current address: Institut IMCN, Université Catholique Louvain, Place Louis Pasteur 1, B-1348 Louvain-la-Neuve, Belgium.

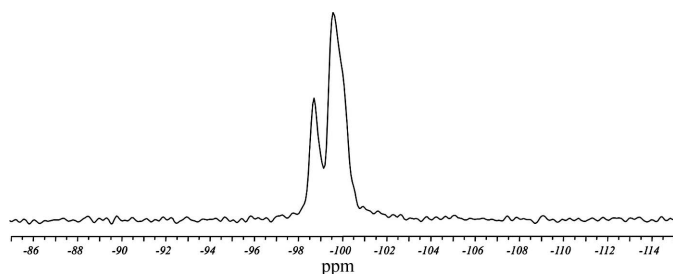


Figure 4
The ^{29}Si MAS NMR spectrum of crystals of (I).

^{29}Si NMR resonances of silicate cubes are generally found around -99.5 p.p.m. The reduced symmetry of the silicate cube can give rise to different local environments, thereby generating different ^{29}Si resonance signals (Harris *et al.*, 1995; Harris & Naumov, 1996; Wiebcke & Koller, 1992; Wiebcke *et al.*, 1993, 1994). Furthermore, a different charge on the terminal O atoms (O^- versus OH) could also result in small differences in the NMR frequency of the Si atoms. Therefore, the ^{29}Si MAS NMR spectrum of (I) can be explained by the presence of a single type of anionic silicate cube with a reduced symmetry, confirming the results obtained from single-crystal diffraction experiments.

Experimental

Adamantyltrimethylammonium hydroxide (TMAdaOH) was prepared by ion exchange from the iodide, which was obtained by reaction of 1-adamantylamine (Acros, 99%) with an excess of methyl iodide (Acros, 99%), according to the procedure of Zones (1985). Silicate hydrate crystals were synthesized at room temperature from a clear solution, prepared by adding tetraethyl orthosilicate (TEOS; Acros, 98%) with vigorous stirring to a 0.7 M aqueous solution of TMAdaOH. The clear solution was then stirred continuously until crystals of (I) formed. The ^{29}Si MAS NMR spectrum was recorded on a Bruker AMX300 spectrometer. 4000 scans with a recycle delay of 60 s were accumulated.

Crystal data

$6\text{C}_{13}\text{H}_{24}\text{N}^+\cdot\text{H}_2\text{O}_{20}\text{Si}_8^{6-}\cdot 44\text{H}_2\text{O}$	$\gamma = 82.119$ (2) $^\circ$
$M_r = 2505.44$	$V = 3356.8$ (3) \AA^3
Triclinic, $P\bar{1}$	$Z = 1$
$a = 15.5889$ (8) \AA	Cu $K\alpha$ radiation
$b = 15.9297$ (8) \AA	$\mu = 1.53$ mm^{-1}
$c = 16.2269$ (11) \AA	$T = 100$ K
$\alpha = 60.863$ (2) $^\circ$	$0.24 \times 0.24 \times 0.10$ mm
$\beta = 72.511$ (3) $^\circ$	

Data collection

Bruker SMART 6000 diffractometer	66631 measured reflections
Absorption correction: multi-scan (SADABS; Bruker, 1997)	12596 independent reflections
$T_{\min} = 0.587$, $T_{\max} = 0.858$	10388 reflections with $I > 2\sigma(I)$
	$R_{\text{int}} = 0.041$

Refinement

$R[F^2 > 2\sigma(F^2)] = 0.065$	399 restraints
$wR(F^2) = 0.186$	H-atom parameters constrained
$S = 1.07$	$\Delta\rho_{\max} = 0.90$ e \AA^{-3}
12596 reflections	$\Delta\rho_{\min} = -0.69$ e \AA^{-3}
942 parameters	

The crystal structure displays a high degree of disorder of the template molecules. Of the three TMAda cations in the asymmetric unit, only one shows no disorder. A second molecule is present in two conformations [refined occupancy = 0.522 (6):0.478 (6) for adamantane and 0.559 (22):0.441 (22) for trimethylammonium], rotated approximately 60° around the N–adamantyl bond. The third cation shows threefold disorder, also around the N–adamantyl bond (occupancies were fixed at 0.333). The adamantane substructures of this threefold disordered TMAda cation were refined to target values provided by the undisordered one. Distance restraints were set-up with a standard deviation of 0.01 \AA and the standard deviation on the angle restraints, expressed as 1,3-distances, was set at twice this value (0.02 \AA). No distance or angle restraints were applied to the second cation showing twofold disorder. Rigid-bond restraints on the anisotropic displacement parameters (standard deviation = 0.005 \AA^2) were applied within every part of the threefold disordered adamantane substructure and simultaneously the same anisotropic displacement parameters were used for all corresponding atoms in the three disordered parts. Moreover, the individual thermal displacement components of the threefold disordered adamantane are refined to approximate to isotropic behaviour (standard deviation = 0.01 \AA^2). The same anisotropic displacement parameters were used for the C atoms of the two parts of the trimethylammonium group attached to the threefold disordered adamantane substructure (the C

Table 1

Hydrogen-bond geometry (\AA , $^\circ$).

$D-H\cdots A$	$D-H$	$H\cdots A$	$D\cdots A$	$D-H\cdots A$
O4–H4 \cdots O29 ⁱ	0.84	1.84	2.659 (4)	166
O21–H21D \cdots O1 ⁱ	0.84	1.83	2.664 (3)	173
O21–H21E \cdots O23	0.84	1.94	2.775 (3)	174
O22–H22D \cdots O9 ⁱⁱ	0.84	1.82	2.647 (3)	169
O22–H22E \cdots O36 ⁱⁱ	0.84	1.98	2.809 (3)	172
O23–H23D \cdots O9 ⁱ	0.84	1.79	2.631 (3)	177
O23–H23E \cdots O40 ⁱ	0.84	1.93	2.758 (3)	167
O24–H24D \cdots O7 ⁱⁱⁱ	0.84	1.78	2.618 (3)	172
O24–H24E \cdots O22	0.84	1.89	2.725 (3)	172
O25–H25D \cdots O7 ⁱⁱⁱ	0.84	1.85	2.689 (3)	176
O25–H25E \cdots O38	0.84	2.02	2.831 (3)	163
O26–H26D \cdots O7	0.84	1.91	2.710 (3)	160
O27–H27D \cdots O28	0.84	1.92	2.750 (3)	173
O27–H27E \cdots O25 ⁱⁱⁱ	0.84	1.96	2.794 (3)	174
O28–H28D \cdots O24 ⁱⁱⁱ	0.84	1.90	2.729 (3)	171
O28–H28E \cdots O24 ^{iv}	0.84	1.90	2.737 (3)	172
O29–H29D \cdots O31	0.84	1.88	2.699 (3)	163
O29–H29E \cdots O37	0.84	2.01	2.802 (3)	157
O30–H30D \cdots O41 ⁱⁱⁱ	0.84	2.03	2.763 (3)	145
O31–H31E \cdots O1 ⁱ	0.84	1.91	2.665 (3)	149
O32–H32D \cdots O33	0.84	1.91	2.749 (3)	175
O32–H32E \cdots O4 ^v	0.84	2.01	2.831 (4)	164
O33–H33D \cdots O42 ⁱ	0.84	2.13	2.737 (3)	129
O33–H33E \cdots O9 ⁱⁱ	0.84	1.97	2.710 (4)	147
O34–H34D \cdots O30	0.84	1.88	2.712 (3)	170
O34–H34E \cdots O33	0.84	1.94	2.774 (3)	174
O35–H35D \cdots O21	0.84	1.94	2.783 (3)	176
O35–H35E \cdots O34	0.84	2.01	2.785 (3)	154
O36–H36E \cdots O27	0.84	1.90	2.734 (3)	171
O37–H37E \cdots O39 ^{vi}	0.84	1.96	2.723 (3)	150
O38–H38E \cdots O1 ^v	0.84	1.90	2.691 (3)	156
O39–H39D \cdots O4	0.84	1.91	2.744 (3)	170
O39–H39E \cdots O26	0.84	1.91	2.751 (3)	175
O40–H40D \cdots O23 ^{iv}	0.84	1.91	2.742 (3)	175
O40–H40E \cdots O36	0.84	1.84	2.647 (3)	161
O41–H41D \cdots O28	0.84	1.88	2.716 (3)	178
O41–H41E \cdots O26	0.84	1.99	2.779 (3)	156
O42–H42D \cdots O40	0.84	1.78	2.614 (3)	175
O42–H42E \cdots O35 ⁱ	0.84	2.00	2.840 (3)	177

Symmetry codes: (i) $-x+1, -y+1, -z+1$; (ii) $x-1, y, z$; (iii) $-x+1, -y+1, -z$; (iv) $x+1, y, z$; (v) $-x+1, -y, -z+1$; (vi) $x, y+1, z$.

atoms of one disordered part are refined without thermal displacement restraints, while the other disordered part is pairwise given the same displacement parameters). The twofold disordered methyl groups of the trimethylammonium group attached to the threefold disordered adamantane were refined with site-occupation factors of 0.455 (6):0.545 (6).

The silanol H atom was located in a difference map, as were the majority of the water H atoms. These H atoms were, after location in a difference map, fixed on their parent O atoms and the water molecules were refined as rigid groups, with the H atoms as dependent atoms able to rotate around and move with their O atoms, while retaining an idealized geometry. For the remaining water H atoms that could not be unequivocally located, the H-atom position was chosen to optimize the hydrogen-bond network, and again the water molecules were treated as above. For all H atoms, $U_{\text{iso}}(\text{H}) = 1.2U_{\text{eq}}(\text{parent atom})$ or $1.5U_{\text{eq}}(\text{C})$ for methyl groups. The solvent water O—H bonds were fixed at 0.84 Å, with a 108° angle between them. The reported hydrogen-bond H...A distances are in the range 1.78–2.12 Å and the hydrogen-bond D—H...A angles are in the range 129.2–177.2°; average values are 1.92 Å and 165.2°, respectively, for 39 observed hydrogen bonds.

Part of the solvent, 55 electrons (presumably water or ethanol molecules), in a cavity of 158 Å³ centred about an inversion centre, could not be modelled and was treated with the SQUEEZE procedure in PLATON (Spek, 2009). This solvent has not been included in the reported empirical formula, M_r , $F(000)$, calculated density or linear absorption coefficient.

Data collection: SMART (Bruker, 1997); cell refinement: SAINT (Bruker, 1997); data reduction: SAINT; program(s) used to solve structure: SHELXS97 (Sheldrick, 2008); program(s) used to refine structure: SHELXL97 (Sheldrick, 2008); molecular graphics: PLUTON (Spek, 2009); software used to prepare material for publication: PLATON (Spek, 2009).

PLHV acknowledges the Flemish IWT for a PhD grant. KR acknowledges the Research Fund of the Katholieke Universiteit Leuven for a postdoctoral position. Kristof Houthoofd is

greatly acknowledged for the ²⁹Si MAS NMR measurements. This work was supported by the Flemish Government via long-term structural funding (Methusalem) and Concerted Research Action (GOA), and by the Belgian Government via IAP-PAI.

Supplementary data for this paper are available from the IUCr electronic archives (Reference: SF3136). Services for accessing these data are described at the back of the journal.

References

- Benner, K., Klüfers, P. & Schuhmacher, J. (1997). *Angew. Chem. Int. Ed. Engl.* **36**, 743–745.
- Bissert, G. & Liebau, F. (1987). *Z. Kristallogr.* **179**, 357–371.
- Bruker (1997). *SADABS* (Version 2.10), *SMART* (Version 5.625) and *SAINTE* (Version 5/6.0). Bruker AXS Inc., Madison, Wisconsin, USA.
- Emmer, J. & Wiebcke, M. (1994). *Chem. Commun.* pp. 2079–2080.
- Grube, M., Wiebcke, M., Felsche, J. & Engelhardt, G. (1993). *Z. Anorg. Allg. Chem.* **619**, 1098–1104.
- Harris, R. K., Howard, J. A. K., Samadi-Maybody, A. & Yao, J. W. (1995). *J. Solid State Chem.* **120**, 231–237.
- Harris, R. K. & Naumov, Y. D. (1996). *J. Chem. Soc. Dalton Trans.* pp. 3349–3355.
- Shantz, D. & Lobo, R. F. (2001). *Microporous Mesoporous Mater.* **43**, 127–136.
- Sheldrick, G. M. (2008). *Acta Cryst.* **A64**, 112–122.
- Smolin, Y. I. (1970). *Sov. Phys. Crystallogr.* **15**, 23–27.
- Spek, A. L. (2009). *Acta Cryst.* **D65**, 148–155.
- Verlooy, P. L. H., Robeyns, K., Van Meervelt, L., Lebedev, O. I., Van Tendeloo, G., Martens, J. A. & Kirschhock, C. E. A. (2010). *Microporous Mesoporous Mater.* **130**, 14–20.
- Wiebcke, M. (1991). *Chem. Commun.* pp. 1507–1508.
- Wiebcke, M., Emmer, J. & Felsche, J. (1995). *Microporous Mater.* **4**, 149–158.
- Wiebcke, M., Emmer, J., Felsche, J., Hoebbel, D. & Engelhardt, G. (1994). *Z. Anorg. Allg. Chem.* **620**, 757–765.
- Wiebcke, M. & Felsche, J. (2001). *Microporous Mesoporous Mater.* **43**, 289–297.
- Wiebcke, M., Grube, M., Koller, H., Engelhardt, G. & Felsche, J. (1993). *Microporous Mater.* **2**, 55–63.
- Wiebcke, M. & Koller, H. (1992). *Acta Cryst.* **B48**, 449–458.
- Zones, S. I. (1985). US Patent No. 4544538.